Studying Turbulence Using Numerical Simulation Databases - VI

Proceedings of the 1996 Summer Program

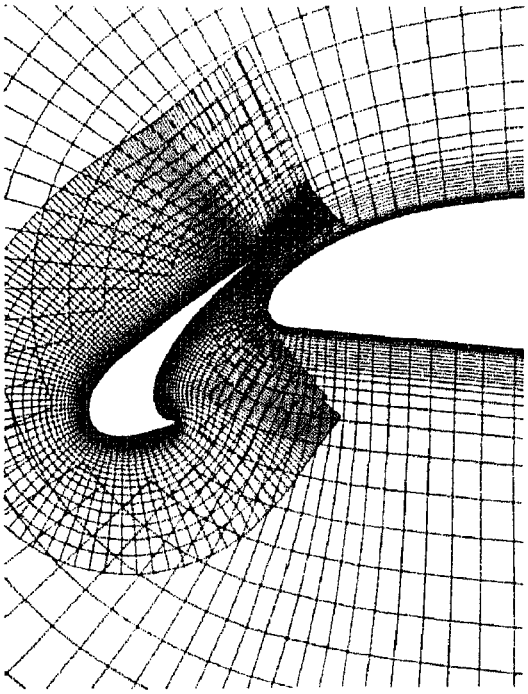

Center for Turbulence Research

December 1996

Ames Research Cente

Stanford University

Asymptotic solution of the turbulent mixing layer for velocity ratio close to unity

By F. J. Higuera[1], J. Jiménez[2] AND A. Liñán[1]

The equations describing the first two terms of an asymptotic expansion of the solution of the planar turbulent mixing layer for values of the velocity ratio close to one are obtained. The first term of this expansion is the solution of the well-known time-evolving problem and the second, which includes the effects of the increase of the turbulence scales in the stream-wise direction, obeys a linear system of equations. Numerical solutions of these equations for a two-dimensional reacting mixing layer show that the correction to the time-evolving solution may explain the asymmetry of the entrainment and the differences in product generation observed in flip experiments.

1. Introduction

Time evolving simulations of the mixing layer are believed to capture many important features of the dynamics of this flow, and are widely used because they are simpler to implement, less expensive, and less subject to uncertainties coming from approximate boundary conditions than the alternative space-evolving simulations. Some features of the real flow, however, are outside the framework of the time-evolving simulations. In particular, it is known that an incompressible mixing layer does not entrain equal amounts of fluid from each of the two free streams (Dimotakis, 1986 and references therein) and that, when the free streams carry passive scalars, the average composition in the molecularly mixed fluid in the mixing layer is nearer to the composition of the fast stream than to the composition of the slow stream. While it is not clear to what extent the second of these features is a consequence of the first or of some asymmetry of the process leading to molecular mixing inside the layer, none of the two can be captured by a time-evolving simulation, owing to the intrinsic symmetry of this artificial flow.

The amount of molecular mixing and the variation of the mixed fluid mean concentration across the layer depend on the Reynolds number, the degree of development of the layer, and the Prandtl or Schmidt number of the scalar; these factors determining in particular the extent to which free stream fluid is transported across the layer by the large scale motions before being molecularly mixed (Konrad 1976; Batt 1977; Mungal & Dimotakis 1984; Koochesfahani & Dimotakis 1986; Karasso & Mungal 1996), but the asymmetries mentioned above occur in any case.

1 E. T. S. Ingenieros Aeronáuticos, UPM, Madrid

2 Center for Turbulence Research

The effect of the scalar field asymmetry is specially obvious when the species carried by the two streams are reactive and lead to a diffusion flame inside the mixing layer, in which a unit of mass of a stream (the fuel stream say) reacts with S units of mass of the other (the oxidizer stream). Then, flip experiments, consisting in exchanging the reactive species between the two streams and keeping constant their concentrations and all the other operating conditions (Mungal & Dimotakis 1984; Koochesfahani & Dimotakis 1986; Karasso & Mungal 1996), clearly show that the amount of product generated by the chemical reaction is larger when the reactant that is more consumed (the oxidizer if $S > 1$) is carried by the fast stream.

To study the effect of these asymmetries, a correction to the time-evolving mixing layer formulation is worked out here using an asymptotic expansion for small differences of the two stream velocities. The analysis follows the lines of Spalart (1986, 1988). The new formulation is applied to a constant density two-dimensional reactive mixing layer with an infinitely fast, diffusion controlled reaction. In this limit, and assuming in addition that the Lewis numbers of the two reactants are equal to one, the chemical reaction can be easily accounted for following the evolution of a linear combination of the mass fractions of the reactants (the mixture fraction Z) which takes the values 0 and 1 in the oxidizer and fuel streams and is transported as a passive scalar. The mass fraction of the product (also with Lewis number equal to one) is a piecewise linear function of Z given by (6) below (see, e.g., Williams 1985).

2. Formulation

The turbulent mixing layer is a statistically stationary flow and, asymptotically, after an adjustment region, it is also statistically self-similar. Our aim here is to try to take advantage of these two properties to simplify the numerical computations.

The large length and time scales of the turbulence are proportional to the streamwise distance x in the self-similar state, and the variation of these scales is inextricably linked to the dynamics of the layer, being brought about by the process responsible for its evolution (vortex pairings in the classical view). This feature makes the numerical simulation costly because a long and wide stretch of the layer must be simulated in order to see the approach to its self-similar state.

The opening angle of the mixing layer is often small. Formally this is true when the velocities of the two streams are close to each other, but in fact the angle is fairly small in any case. On one hand, this feature makes the numerical simulations even more expensive, because a very long stretch is needed to see the initial size of a typical vortex grow by a given factor. On the other hand, this feature is the basis of a well known simplification of the numerical treatment, based on the fact that the changes of time and length scales are small, and can be taken into account as a perturbation, over distances of the order of the size of one or a few vortices.

This is so because for a layer growing by pairings of the large vortices, for which each vortex must undergo a number of these discrete events to approach the self-similar state, a small angle amounts to a small ratio of the size of a vortex to the distance it travels between successive pairings. But then, since the spacing of the large scale vortices is not much larger than their size, there are many neighboring

vortices to the left and to the right of a given vortex with sizes not very different from its own size, and it seems reasonable to think that the evolution of a vortex and of its nearest neighbors between successive pairings depends on the details of the evolution of only a number of other neighbors, whereas the effect of the rest of the mixing layer can be taken into account using a kind of mean field approximation without regard for individual features of the far vortices.

Since the vortices move with a velocity intermediate between the velocities of the two streams, these conditions can be better put to use in a reference frame moving with that intermediate velocity. In this reference frame the evolution of a vortex can be described following the detailed dynamics of the flow over a span containing only a limited number of neighbor vortices. Here, using periodicity conditions in the stream-wise direction amounts, of course, to a temporal simulation of the flow, but the equations describing the small perturbations due to the growth of the turbulent scales can be easily worked out and solved along with those of the temporal simulation. It is worth recalling, however, that a definite error of a different type is always associated to the use of periodic conditions because the self-similarity and stationarity of the flow are statistical properties not applicable to individual realizations. Hopefully, the importance of this error decreases as the number of vortices included in the simulation increases.

Restricting the computations to a finite span in the moving frame imposes a limitation on the time during which the evolution of the flow may be followed, owing to the growth of the vortices. In principle, a long span is required if the initial conditions are not close to the final self-similar state and a large number of pairings is necessary to approach that state. In practice, such a long span could perhaps be avoided carrying out computations on a shorter one for a moderate lapse of time and then replicating the results one or a few times in new adjacent spans, introducing appropriate phase shifts and a slight decrease of resolution before continuing the computation.

Consider then a plane self-similar mixing layer between two incompressible streams with velocities U_1 and $U_2 < U_1$. Assume that $\epsilon = (U_1 - U_2)/(U_1 + U_2) \ll 1$ to ensure that the angle of the layer, defined in any convenient way, is small of $O(\epsilon)$, though, as was mentioned before, this angle is probably small for any ϵ. The aim is to follow the evolution of a few adjacent vortices, of initial characteristic size δ say, during a time of order $t_c = 2\delta/(U_1 - U_2)$ corresponding to a few pairings. The growth of the mixing layer thickness is taken into account switching to the variables (x^*, η, z^*), where $\eta = y^*/(\epsilon x^*)$ and (x^*, y^*, z^*) are the usual Cartesian coordinates. The statistical properties of the flow imply then that the x-averages coincide with the time averages and both are functions of η only. Next, introducing a reference frame moving with velocity $U_m = (U_1 + U_2)/2$, the solution is sought in the form

$$\mathbf{v}^* = U_m(\mathbf{i} + \epsilon\mathbf{v}), \quad p^* = \rho U_m^2 \epsilon^2 p, \qquad \text{with} \quad x^* = U_m t_c(t + \epsilon x), \tag{1}$$

where the non-dimensional variables $(\mathbf{v}, p)$ are of order unity and the distances and time are scaled with δ and t_c, respectively. In terms of these variables the

Navier-Stokes equations and the equation for the mixture fraction are

$$\left.\begin{aligned} G_i v_i - \frac{\epsilon\eta}{t+\epsilon x}\partial_\eta u = 0 \\ \partial_t v_i + (\tilde{v}_i G_i) v_i = -G_i p + \frac{1}{Re}\nabla^2 v_i \\ \partial_t Z + (\tilde{v}_i G_i) Z = \frac{1}{RePr}\nabla^2 Z \end{aligned}\right\} , \tag{2}$$

where $\mathbf{G} = (\partial_x,\, 1/(t+\epsilon x)\,\partial_\eta,\, \partial_z)$ is a symbolic vector, $\tilde{\mathbf{v}} = (u, v-\eta(1+\epsilon u), w)$, the Laplacian operator acting on each component of the velocity is $\nabla^2 = \partial_{xx} + (1+\epsilon^2\eta^2)/(t+\epsilon x)^2\partial_{\eta\eta} + \partial_{zz} - 2\epsilon\eta/(t+\epsilon x)\partial_{x\eta} + 2\epsilon^2\eta/(t+\epsilon x)^2\partial_\eta$, $Re = (U_1 - U_2)\delta/2\nu$, and Pr is the Prandtl number. The solution of (2) can be sought as a power series in ϵ, of the form $(\mathbf{v},\, p,\, Z) = (\mathbf{v}_0,\, p_0,\, Z_0) + \epsilon(\mathbf{v}_1,\, p_1,\, Z_1) + \cdots$.

Carrying this expansion into (2) we find, at leading order,

$$\left.\begin{aligned} G_{0_i} v_{0_i} = 0 \\ \partial_t v_{0_i} + (\tilde{v}_{0_j} G_{0_j}) v_{0_i} = -G_{0_i} p_0 + \frac{1}{Re}\nabla_0^2 v_{0_i} \\ \partial_t Z_0 + (\tilde{v}_{0_j} G_{0_j}) Z_0 = \frac{1}{RePr}\nabla_0^2 Z_0 \end{aligned}\right\} , \tag{3}$$

where $\mathbf{G}_0 = (\partial_x,\, 1/t\,\partial_\eta,\, \partial_z)$, $\tilde{\mathbf{v}}_0 = (u_0,\, v_0 - \eta,\, w_0)$, and $\nabla_0^2 = \partial_{xx} + 1/t^2\partial_{\eta\eta} + \partial_{zz}$.

At the next higher order linear equations are obtained for $(\mathbf{v}_1, p_1, Z_1)$ having some forcing terms proportional to x (arising from the expansion of the denominators in (2)) and other that do not contain x explicitly. The solution of these equations is of the form $(\mathbf{v}_1, p_1, Z_1) = x\,(\mathbf{v}_{10}, p_{10}, Z_{10}) + (\mathbf{v}_{11}, p_{11}, Z_{11})$, where, as can be easily verified, $(\mathbf{v}_{10}, p_{10}, Z_{10}) = \partial_t(\mathbf{v}_0, p_0, Z_0)$ in order for the time averages to be independent of x, and $(\mathbf{v}_{11}, p_{11}, Z_{11})$ satisfy

$$\left.\begin{aligned} G_{0_i} v_{11_i} + \partial_t u_0 - \frac{\eta}{t}\partial_\eta u_0 = 0 \\ \partial_t v_{11_i} + (\tilde{v}_{0_j} G_{0_j}) v_{11_i} + (\tilde{v}_{11_j} G_{0_j}) v_{0_i} = -G_{0_i} p_{11} + \frac{1}{Re}\nabla_0^2 v_{11_i} + F_i \\ \partial_t Z_{11} + (\tilde{v}_{0_j} G_{0_j}) Z_{11} + (\tilde{v}_{11_j} G_{0_j}) Z_0 + u_0 \partial_t Z_0 - \frac{\eta u_0}{t}\partial_\eta Z_0 = \\ \qquad \frac{1}{RePr}\left(\nabla_0^2 Z_{11} + 2\partial_{xt} Z_0 - \frac{2\eta}{t}\partial_{x\eta} Z_0\right) \end{aligned}\right\} , \tag{4}$$

where $\mathbf{F} = -u_0\partial_t\mathbf{v}_0 + \eta u_0/t\,\partial_\eta\mathbf{v}_0 + 2/Re(\partial_{xt}\mathbf{v}_0 - \eta/t\,\partial_{x\eta}\mathbf{v}_0) + (-\partial_t p_0 + \eta/t\,\partial_\eta p_0,\, 0,\, 0)$. The velocity at this order is therefore $\mathbf{v} = \mathbf{v}_0 + \epsilon(x\,\partial_t\mathbf{v}_0 + \mathbf{v}_{11})$, which can be written as $\mathbf{v}_0(x, \eta, t+\epsilon x) + \epsilon\mathbf{v}_{11}$, and the pressure and mixture fraction are analogous. The first term admits a simple interpretation: as far as it is concerned the state of development of the flow is proportional to x, being slightly more evolved downstream of a point than it is upstream. Thus, even if periodic boundary conditions are used as an approximation for the leading order problem (3), as will be done in the

following section, this first term is not periodic. The effect of the second term will be discussed later.

Applying x- and t-averages in suitable order to Eqs. (3) and to the continuity equation in (4) yields

$$\left.\begin{aligned} \frac{d\overline{v}_0}{d\eta} &= 0 \\ \frac{d}{d\eta}(\overline{u_0 v_0}) - \eta\frac{d\overline{u}_0}{d\eta} &= 0 \\ \frac{d}{d\eta}(\overline{v_0^2} + \overline{p}_0) &= 0 \\ \frac{d}{d\eta}(\overline{u_0 Z_0}) - \eta\frac{d\overline{Z}_0}{d\eta} &= 0 \\ \frac{d\overline{v}_{11}}{d\eta} - \eta\frac{d\overline{u}_0}{d\eta} &= 0 \end{aligned}\right\} , \tag{5}$$

where the bars denote averaged variables. The first of these equations gives $\overline{v}_0 = 0$ (a constant v_0 has no effect on the dynamics; it can be set equal to zero by an $O(\epsilon)$ change in the orientation of the x axis). The last equation in (5) implies that the mean normal velocity is of order ϵ relative to the variation of the streamwise velocity, as could have been expected for a region of $O(\epsilon)$ aspect ratio. Using the second equation to eliminate $\eta\, d\overline{u}_0/d\eta$ and integrating, this equation yields $\overline{v}_{11} - \overline{u_0 v_0} =$ constant. Since $\overline{u_0 v_0} = 0$ for $\eta \to \pm\infty$, the normal velocity v_{11} tends to the same constant value on both sides of the mixing layer, and this constant can be set equal to zero as for v_0. Therefore the mixing layer does not introduce any perturbation in the free streams to this order and the ingestion of fluid by the layer is due only to the linear growth with x of its upper and lower apparent boundaries.

Since the orientation of the x-axis is well determined by the conditions $v_0 = v_1 = 0$ outside the mixing layer, the upper and lower boundaries can be defined on the basis of the usual thicknesses. For example, using the scaled momentum thickness $\Delta_m = \int_{-\infty}^{\infty} \overline{(U_1 - u^*)(u^* - U_2)}\, dy^*/[\epsilon x^*(U_1 - U_2)^2]$ and the scaled product thickness $\Delta_p = \int_{-\infty}^{\infty} \overline{Y_p(Z)}\, dy^*/(\epsilon x^*)$, where $Y_p(Z)$ is the product mass fraction given by the piecewise linear function

$$Y_p = \begin{cases} Z/Z_s & \text{for} \quad 0 \le Z \le Z_s \\ (1-Z)/(1-Z_s) & \text{for} \quad Z_s \le Z \le 1 \end{cases} \tag{6}$$

with $Z_s = 1/(1+S)$, the scaled upper and lower boundaries are

$$\begin{aligned} \Delta_m^{\pm} &= \pm\frac{1}{4}\int_0^{\pm\infty} (1 - \overline{u^2})\, d\eta = \pm\frac{1}{4}\int_0^{\pm\infty} (1 - \overline{u_0^2})\, d\eta \mp \frac{\epsilon}{2}\int_0^{\pm\infty} \overline{u_0 u_{11}}\, d\eta + \cdots \\ \Delta_p^{\pm} &= \pm\int_0^{\pm\infty} \overline{Y_p(Z)}\, d\eta \end{aligned} \tag{7}$$

and $\Delta_m = \Delta_m^+ + \Delta_m^-$, $\Delta_p = \Delta_p^+ + \Delta_p^-$.

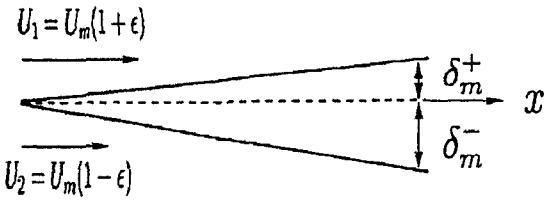

FIGURE 1. Sketch of the apparent boundaries and entrainment process.

3. Results

The two-dimensional forms of Eqs. (3) and (4) were numerically solved to find the effect of the first order corrections on the growth rate and the asymmetry of the layer. For this purpose the variable $y = \eta t$, which is the non-dimensional normal distance divided by the factor $1 + \epsilon x/t$, was used instead of η. The equations then take the form

$$\left.\begin{aligned} \nabla \cdot \mathbf{v}_0 &= 0 \\ \partial_t \mathbf{v}_0 + \nabla \cdot (\mathbf{v}_0 \mathbf{v}_0) &= -\nabla p_0 + \frac{1}{Re}\nabla^2 \mathbf{v}_0 \\ \partial_t Z_0 + \nabla \cdot (\mathbf{v}_0 Z_0) &= \frac{1}{RePr}\nabla^2 Z_0 \end{aligned}\right\} \tag{8}$$

$$\left.\begin{aligned} \nabla \cdot \mathbf{v}_{11} &= -\partial_t u_0 \\ \partial_t \mathbf{v}_{11} + \nabla \cdot (\mathbf{v}_0 \mathbf{v}_{11} + \mathbf{v}_{11} \mathbf{v}_0) &= -\nabla p_{11} + \frac{1}{Re}\nabla^2 \mathbf{v}_{11} + \partial_t \mathbf{R} \\ \partial_t Z_{11} + \nabla \cdot (\mathbf{v}_0 Z_{11} + \mathbf{v}_{11} Z_0) &= \frac{1}{RePr}\nabla^2 Z_{11} + \partial_t \left(-u_0 Z_0 + \frac{1}{RePr}\partial_x Z_0 \right) \end{aligned}\right\} \tag{9}$$

with $\mathbf{R} = -u_0 \mathbf{v}_0 + 2/Re\, \partial_x \mathbf{v}_0 - (p_0, 0)$, and were solved with the boundary conditions $\mathbf{v}_0 \mp \mathbf{i} = \mathbf{v}_{11} = Z_{11} = 0$ and $Z_0 = (1, 0)$ for $y \to \pm\infty$, and periodicity conditions in the stream-wise direction. The use of periodicity conditions is an approximation for which the only possible justification seems to be that in the present variables they are compatible with the spatial growth of the turbulence scales, and that, hopefully, they do not distort the solution too much if the period is sufficiently larger than the size of the vortices during most of the simulation. The initial conditions for the leading order variables were the hyperbolic tangent profiles $u_0 = \tanh 2y$ and $Z_0 = \frac{1}{2}(1 + \tanh 2y)$ plus perturbations proportional to the most unstable linear mode and one or two sub-harmonics with different amplitudes and phases. The variables $\mathbf{v}_{11}$ and Z_{11} were initially zero. In the simulations $Pr = 1$ and $Re = 500$-1000, based on the initial vorticity thickness.

With these conditions, $\mathbf{v}_0$, $Z_0 - 1/2$ and p_{11} change sign under the transformation $(x, y, t) \to (-x, -y, t)$ while $\mathbf{v}_{11}$, Z_{11}, and p_0 are left invariant. The mixing layer grows symmetrically in first approximation, leading to $\Delta^+_{m_0} = \Delta^-_{m_0} = \Delta_{m_0}/2$, whereas the correction to the growth rate is antisymmetric: $\Delta^+_{m_1} = -\Delta^-_{m_1}$, $= \Delta_{m_1}$ say (the same relations hold for the product thickness when $S = 1$). Here Δ_{m_0} and Δ_{m_1} are the slopes of straight lines fitted to $\delta_{m_0} = \frac{1}{4}\int_{-\infty}^{\infty}(1 - \overline{u_0^2})\,dy$ and $\delta_{m_1} = -\frac{1}{2}\int_0^{\infty} \overline{u_0 u_{11}}\,dy$. The fluxes crossing the upper and lower apparent boundaries of

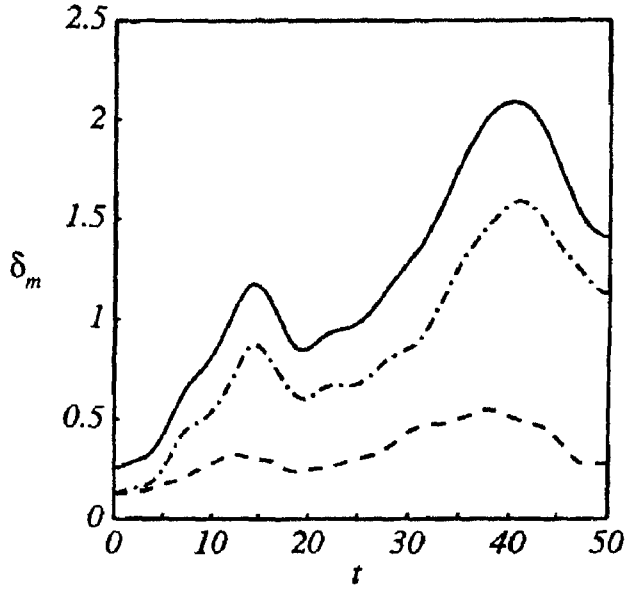

FIGURE 2. Momentum thickness (———) and upper and lower boundaries (---- and —·— , respectively) for $\epsilon = 0.45$ ($r = U_2/U_1 = 0.38$), $Re = 500$ and $Pr = 1$.

the layer, scaled with $\epsilon U_m x^*$, are (see Fig. 1) $\phi^{\pm} = (1 \pm \epsilon)\Delta_m^{\pm} = [\Delta_{m_0} \pm \epsilon(\Delta_{m_0} + 2\Delta_{m_1}) + \cdots]/2$, where the momentum thickness is used for definiteness, and the entrainment ratio, defined here as $E = \phi^+/\phi^-$, is

$$E = 1 + \epsilon\left[1 + 2\frac{\Delta_{m_1}}{\Delta_{m_0}}\right] + O(\epsilon^2). \tag{10}$$

The total momentum thickness $\delta_m = \delta_{m_0}$ and the upper and lower apparent boundaries, $\delta_m^+ = \delta_{m_0}/2 + \epsilon\delta_{m_1}$ and $\delta_m^- = \delta_{m_0}/2 - \epsilon\delta_{m_1}$ respectively, are given in Fig. 2 for a representative case displaying a pairing. The numerical results show that the layer opens more toward the slow stream ($\Delta_{m_1} < 0$), but this effect is overbalanced by the higher speed of the fast stream resulting in a E slightly greater than one.

Figure 3 shows the product thickness for $S = 1$ and for $S = 8$ and $1/8$. The last two values correspond to a flip experiment in which the fuel and the oxidizer streams are exchanged. The results show that the generation of product is higher when the reactant that is more consumed is carried by the fast stream.

Both results are in qualitative agreement with the experimental data. Quantitative comparisons are meaningless given the two-dimensional character of the present simulations.

The explanation of these results can be traced, of course, to the form of the forcing terms on the right hand sides of Eqs. (9). These terms depend only on time derivatives of the leading order solution, and the signs of some of them can be easily guessed. Thus, since the antisymmetric profile of $\overline{u}_0(y)$ (the bar meaning here x-average) gets thicker with time, $-\partial_t u_0$ in the continuity equation is more

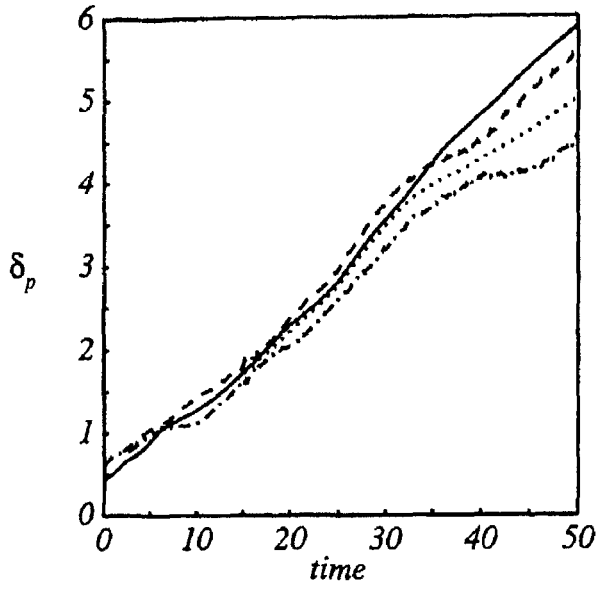

FIGURE 3. Product thickness for $S = 1$ (——— ; not affected by the asymmetry) and for $S = 8$ (—·—) and 1/8 (----), corresponding to a flip experiment, for $\epsilon = 0.45$, $Re = 500$ and $Pr = 1$. ····· : common value for $S = 8$ and 1/8 when $\epsilon = 0$.

often positive than negative in the upper part of the layer, which amounts to a distribution of sources, and vice versa in the lower part, which amounts to sinks.

For the same reason, $-\partial_t u_0^2$ should be positive, on average, everywhere in the layer, and the numerical results show that this is also true of the whole forcing term $-\partial_t(u_0^2 + p_0) + 2/Re\,\partial_{xt} u_0$ in the x-momentum equation. This amounts to a force pushing the fluid in the stream-wise direction and leading to a u_{11} predominantly positive. Therefore the average velocity $\overline{u}_0 + \epsilon\overline{u}_{11}$ approaches its asymptotic value $+1$ in the upper stream faster than its asymptotic value -1 in the lower stream, which explains the results in Fig. 2.

The forcing term in the equation for Z_{11} has a complicated structure with bands of alternate signs. On average, however, it is positive (as could have been expected of the term $-\partial_t(\overline{u_0 Z_0})$, due to the increase of thickness of the profile of $\overline{Z}_0$ with time), leading to a Z_{11} with a banded structure but predominantly positive. Hence the region of $\overline{Z}$ near 1 in the upper part of the layer is wider than the region of $\overline{Z}$ near 0 in the lower part. This provides an explanation for the results in Fig. 3 because the upper region is responsible for a larger fraction of the product than the lower region when S is small and the average position of the flame is shifted toward the upper side, while the lower region is responsible for a larger fraction of the product than the upper region when S is large and the average position of the flame is shifted toward the lower side.

Since the forcing terms depend only on the leading order solution, they could perhaps be evaluated from the results of a three-dimensional time-evolving simulation (as that of Roger & Moser 1994), which would give indications on whether the

above observed trends hold also for that more realistic case.

Finally it may be noted that the condition $\epsilon \ll 1$, used here as the basis of a formal expansion, may not be necessary for some of the results to hold. As was mentioned before, the angle of the layer is moderately small for any value of ϵ because the eddy turn over time is always shorter than the time between pairings, and this alone provides the required scale separation.

REFERENCES

BATT, R. G. 1977 Turbulent mixing of passive and chemically reacting species in a low-speed shear layer. *J. Fluid Mech.* **82**, 53-95.

DIMOTAKIS, P. E. 1986 Two-dimensional shear-layer entrainment. *AIAA J.* **24**, 1791-1796.

KARASSO, P. S. & MUNGAL, M. G. 1996 Scalar mixing and reaction in plane liquid shear layers. *J. Fluid Mech. In press.*

KONRAD, J. H. 1976 An experimental investigation of mixing in two-dimensional turbulent shear flows with applications to diffusion-limited chemical reactions. Ph.D. Thesis, Caltech.

KOOCHESFAHANI, M. M. & DIMOTAKIS, P. E. 1986 Mixing and chemical reactions in a turbulent liquid mixing layer. *J. Fluid Mech.* **170**, 83-112.

MUNGAL, M. G. & DIMOTAKIS, P. E. 1984 Mixing and combustion with low heat release in a turbulent shear layer. *J. Fluid Mech.* **148**, 349-382.

ROGERS, M. M. & MOSER, R. D. 1994 Direct simulation of a self-similar turbulent mixing layer. *Phys. Fluids.* **6**, 903-923.

SPALART, P. R. 1986 Numerical study of sink-flow boundary layers. *J. Fluid Mech.* **172**, 307-328.

SPALART, P. R. 1988 Direct simulation of a turbulent boundary layer up to $Re_\theta = 1410$. *J. Fluid Mech.* **187**, 61-98.

WILLIAMS, F. A. 1985 *Combustion Theory*, 2nd ed. Benjamin/Cumming, Menlo Park, CA.